

SUSPENDED PARTICLE DYNAMICS IN A WELL-MIXED ESTUARY: DEVIATIONS FROM MORPHODYNAMIC EQUILIBRIUM

Díez-Minguito M¹, Ortega-Sánchez M¹, Baquerizo A¹, de Swart HE², Losada MA¹

This paper presents an analysis of turbidity and suspended sediment transport during low river flows in the Guadalquivir river estuary (Spain). The distribution and sources of the suspended particulate matter (SPM) are identified. The analysis of the transport rates allow us to devise a semi-analytical model for transport of SPM in well-mixed estuaries. The model solves the mass balance equation for SPM on a tidally-averaged timescale. The main inputs are the along-channel transport rates and the vertical turbulent diffusion coefficients at several locations. The model is applied to the Guadalquivir estuary, where a comprehensive monitoring network was installed from 2008 to 2011. Its application to this estuary allows to check how the SPM concentrations in different reaches of the estuary deviate from their equilibrium values. The results indicate that erosion is dominant in the stretches near to the mouth and that the estuary seems to move towards equilibrium during weak tidal forcing conditions.

Keywords: Guadalquivir Estuary, Suspended Sediment Transport; Estuarine Turbidity Maxima; Box Model; Morphodynamic Equilibrium

INTRODUCTION

The Guadalquivir estuary normally suffers moderate-to-high SPM concentrations, and has water quality problems throughout the year. Turbidity, understood as a tracer of SPM concentrations, typically results in a reduction of light transmission for photosynthesis by phytoplankton in the water column (Talke et al., 2009). In the Guadalquivir estuary, high-turbidity, hypoxic conditions are specially severe after sudden increases in freshwater discharges of short duration. This frequently gives rise to an anoxic water column causing a significant reduction in primary production (Ruiz et al., 2014). Furthermore, fluvio-tidal processes provoke erosion in some stretches whereas in others the risk of shoaling is increased. Periodic dredging works are thus needed to maintain the minimum safety requirements of the navigation channel of the Port of Sevilla (Fig. 1). These works, in turn, also deviate the channel from morphodynamic equilibrium and may trigger higher levels of turbidity. Within this overall context, the recent proposal of channel deepening to allow larger ships to reach the Port of Sevilla, and the management of the discharges from the upstream dam at Alcalá del Río have raised concerns regarding the long-term stability of the estuary.

In order to analyze the current morpho-hydrodynamic status of the estuary, to assess the impact of human interventions and natural forcings, and to help to regulate the different economic and environmental uses, a research study was conducted from 2008 to 2011. The study included the installation of a real-time remote monitoring network which involved a significant deployment of equipment (see Navarro et al. (2011) for details). The stations, operated by the Institute of Marine Sciences of Andalusia (ICMAN-CSIC), were positioned along the estuary and its mouth (see locations in Fig. 1). Among other variables, elevations, currents, salinity, and turbidity were measured.

The analysis of the data recorded by the monitoring network, complemented by the results of a semi-analytical box model for the (tidally-averaged) transport of SPM, permits the identification of the sediment sources and how is the SPM distributed and transported along the estuary. In particular, this analysis allowed for the assessment of the morphological status of the system by estimating how each stretch of the estuary deviates from equilibrium conditions. The results of these analysis are presented in this paper.

A FIRST PICTURE

The Guadalquivir River estuary is located in the SW of the Iberian Peninsula, facing to the Gulf of Cádiz, Atlantic Ocean (Fig. 1). It extends as far as the Alcalá del Río dam, 110 km upstream from the mouth at Sanlúcar de Barrameda. The estuary is dynamically narrow and weakly convergent. The along-channel mean water depth is about 7 m, maintained in most stretches by periodic dredging works. Tides are mesotidal and semidiurnal, being the most important constituent the M2. The dam at Alcalá del Río is the upstream boundary, i.e. the last monitoring point of the freshwater discharges and the up-estuary tidal propagation limit. The bed of the upper reach of the estuary is over 90% composed of fine-grained muds, while in the rest of the estuary a typical distribution is 80% of sand and 20% of silt and clay. The concentration of solids in suspension usually varies between 0.5 kg/m³ and 4.5 kg/m³. Values at the near-surface

¹Andalusian Institute for Earth System Research, University of Granada, Granada, Spain

²Institute for Marine and Atmospheric Research Utrecht, Utrecht University, Utrecht, Netherlands

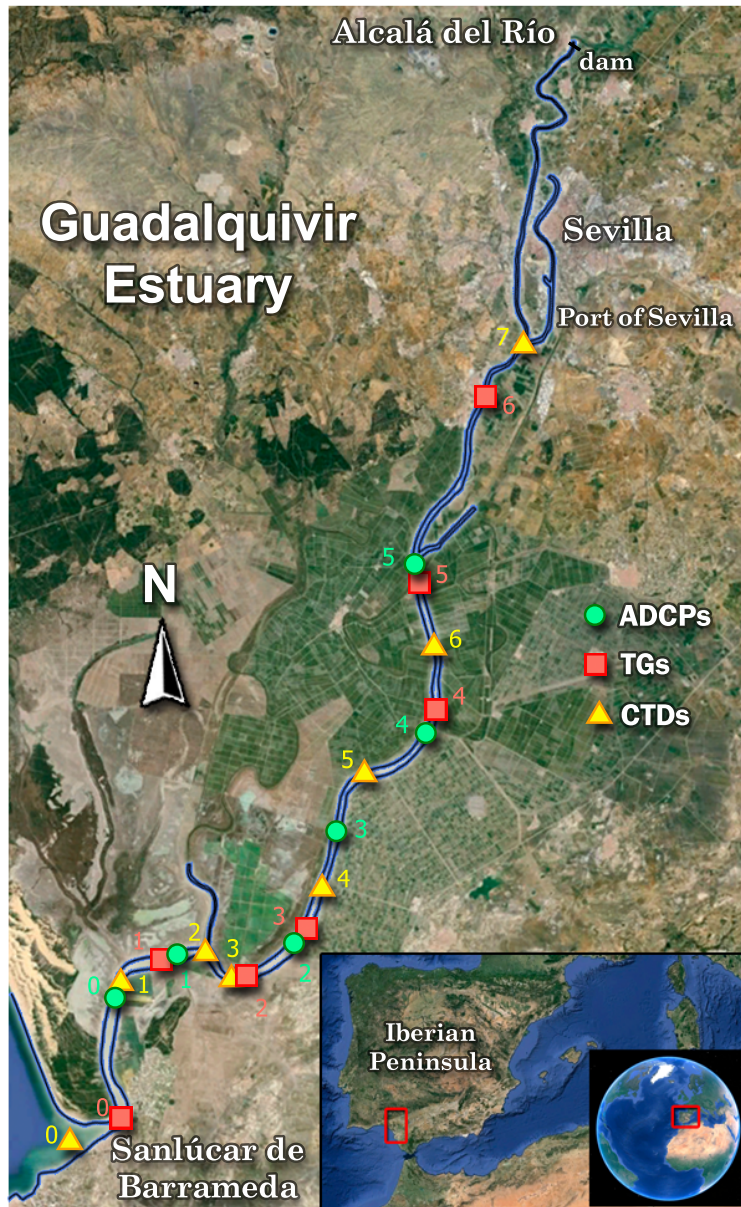


Figure 1: Guadalquivir River Estuary ($(-6.434, -5.821)^{\circ}\text{W}-(36.743, 37.537)^{\circ}\text{N}$) and stations of the monitoring network installed from 2008 to 2011. Data from six current-meter profilers (ADCPs, green circles), seven tidal gauges (TGs, red squares), and eight environmental quality probes or (CTDs, yellow triangles) are used for this work. Background pictures are adapted from Google Earth.

as high as 16 kg/m^3 , triggered by discharges from the upstream dam, have been also found (Contreras and Polo, 2012).

Time series analysis of CTD's measurements (triangles in Fig. 1) revealed the existence of two turbidity regimes, which depend to a great extent on the freshwater discharge regime. When the river discharges released by the upstream dam are lower than approx. $40 \text{ m}^3/\text{s}$, the estuary behaves as a tidally-energetic estuary (Díez-Minguito et al., 2012): the water column is well-mixed (see Fig. 2, bottom panel), but shows a weak vertically-sheared circulation, more evident near the mouth. During these conditions, turbidity values vary in accordance with the ebb-flood and spring-neap cycles. Tidally-averaged concentration values range always below 3 kg/m^3 in all the stations, and two Estuarine Turbidity Maxima (ETM) develop (see below). Most of the results of this paper correspond to this regime.

The other regime, an extreme one, typically triggered by discharge events from the headwater dam, is transitory and presents turbidity values of one or several higher orders of magnitude than the former in practically the whole of the estuary. When discharges are one order of magnitude greater, the estuary is fluviially-dominated. Under that conditions, the salt intrusion reaches the estuary mouth where stratification increases, and a salt-wedge forms. The discharge changes the SPM distribution and one of the ETM is shifted seawards due to the increase in the stratification downstream (Burchard and Baumert, 1998; Lin and Kuo, 2001). Relaxation times towards the normal regime for turbidity take from weeks to several months.

ORIGIN AND DISTRIBUTION OF THE SUSPENDED SEDIMENT

Figure 2 shows typical temporal series of near-surface and near-bottom turbidity, along-channel current, and salinity in the middle part of the estuary. The intratidal variations, namely, the semi-diurnal and quarti-diurnal, are evident in Fig. 2. The correlation between SPM concentrations and flood-ebb currents points to a mainly tidal generation of turbidity. The resuspension capacity of the bed material into the water column by tidally-induced turbulence is lesser during the ebb cycle. This is consistent with a flood-dominated estuary. The tidal asymmetry is clearly visible in the magnitude of the longitudinal current (central panel).

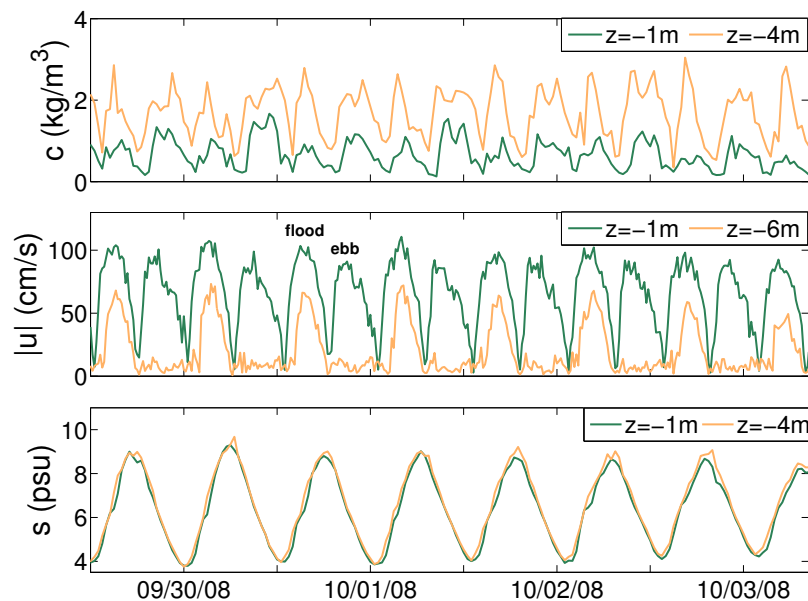


Figure 2: Top panel: Suspended sediment concentration recorded at station CTD4 at $z = -1 \text{ m}$ and $z = -4 \text{ m}$ from the free surface. Central panel: Magnitude of the longitudinal current at station ADCP3 at $z = -1 \text{ m}$ and $z = -6 \text{ m}$. Bottom panel: salinity at station CTD4 at $z = -1 \text{ m}$ and $z = -4 \text{ m}$.

The amount of sediment suspended in the water column (top panel) lags respect to current (central panel), being higher soon after maximum ebb (ME), and, especially, after the maximum flood (MF) (see also Fig. 3). The phase lags between the oscillatory part of the SPM concentration and the tidal current at

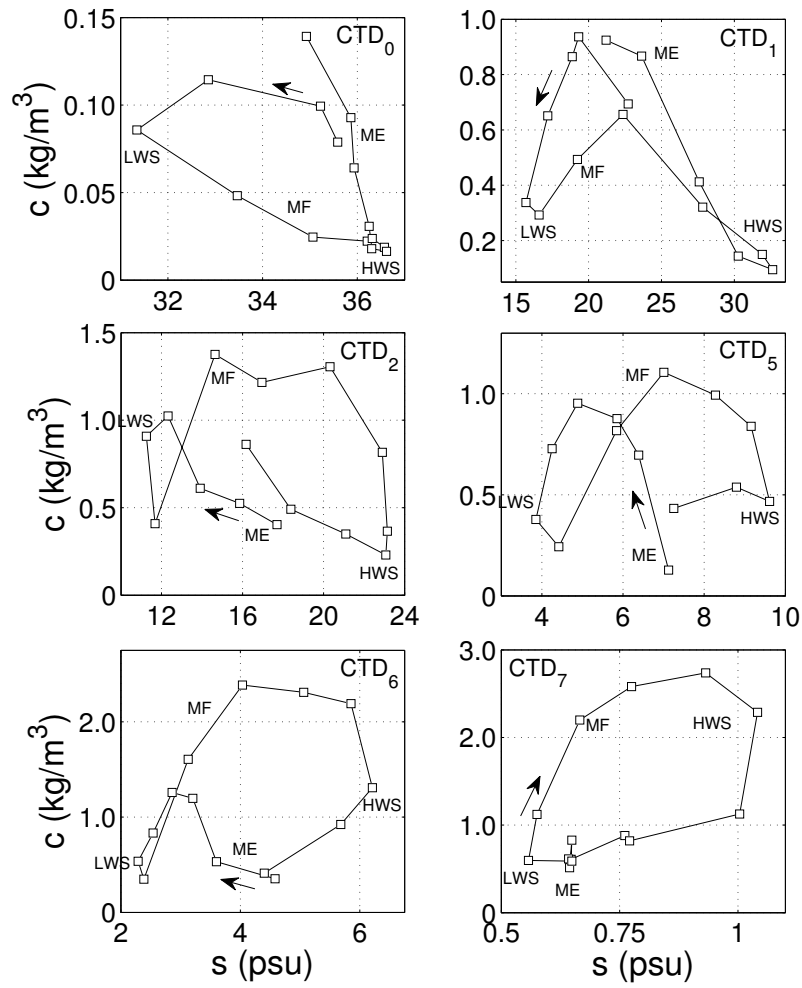


Figure 3: Lissajous curves for salinity (s) and turbidity (c) at the near surface during a tidal cycle at spring tide (08/01/2008) at the stations indicated in each panel. Labels indicate the state of the tide (see definition in main text). Time arrows are included for clarity.

different layers of the water column have important consequences in the residual sediment transport (see below). The harmonics present in the wave forms and their relative phases, which are caused by the complex interaction between flow and solute concentration, often conceptualized in threshold, erosion, scour, and settling lags (Dyer, 1995), are better appreciated by means of Lissajous curves. Figure 3 shows $s - c$ diagrams at the near-surface at different stations.

As shown in Fig. 3, at all locations, the maximum salinity value within a tidal cycle is attained during high water slack (HWS). Conversely, the minimum salinity occurs near low water slack (LWS). However, the maxima and minima SPM concentration values are out of phase with s since the sediment does not respond as fast as s to the flow, and is also entrained locally. The sediment is resuspended by the tidal action twice in a tidal cycle, thus $s - c$ diagrams generally exhibit two lobes (ratio $\omega_{M4}/\omega_{M2} = 2$). This is indeed the case of stations located in the middle part of the estuary, e.g. CTD2 and 5 (Fig. 3, left and right central panels). The highest c values at both stations (1.4 kg/m^3 and 1.1 kg/m^3 , respectively) are attained after MF due to the flood-dominance. The lags between MF and maximum c , as well as the settling lags after HWS and LWS, are lower than 30 min, which is the sampling period. Larger phase shifts (~ 90 min) are observed after ME. According to these lags, the time scale for the vertical diffusivity is $\sim 10^{-3} \text{ m}^2/\text{s}$, similarly to those obtained in Reyes-Merlo et al. (2013).

Diagrams for CTD1 and CTD6 represent transitional configurations between one and two-lobed shapes. The lowermost and uppermost stations (CTD0 and CTD7, respectively) exhibit single-lobed shapes (Fig. 3). At station CTD0, located at the estuary mouth, the lowest c value occurs at HWS, whereas the maximum of c is attained after ME, in spite of that the larger currents occur during the flood phase. This behavior is due to tidal straining (Simpson et al., 1990), which plays an important role in shaping estuarine circulation (Jay and Musiak, 1994). During ebb, seaward flow near the surface advects lighter and more turbid waters. At LWS, a significant amount of suspended sediment settles and c is reduced. During flood, vertical mixing increases and saltier and cleaner waters are directed landward further reducing c . Station CTD7 shows the complementary behavior. The shape is tilted rightwards and the lowest (highest) turbidity value is observed near LWS (one hour after MF). This behavior might also be attributed to correlations between eddy viscosity and vertical shear of the along-channel current. Although no measurements were taken upstream CTD7, the turbidity is lower upstream of this station as can be inferred from the $s - c$ curve at CTD7. In fact, according to the c values shown in Fig. 3, the largest turbidity maximum occurs around CTD7, and another, secondary one appears near CTD2. The analysis of the transports indicate that the ETM are located close to the convergence zones of the sum of M2- and M4-induced tidal pumping transports, $T_{M2} + T_{M4} = \overline{\overline{hu}_{M2}c_{M2}} + \overline{\overline{hu}_{M4}c_{M4}}$. Here, the overline represents the semidiurnal average, and the underline the depth average. Amplitudes and phases of the M2 and M4 constituents are obtained from standard harmonic analysis (Pawlowicz et al., 2002) and used to compute T_{M2} and T_{M4} (Chernetsky et al., 2010).

DEVIATIONS FROM MORPHODYNAMIC EQUILIBRIUM

How is the sediment transported between different stretches along the estuary? To answer this question, the morphological status of the system is assessed. This is carried out by estimating how each stretch of the estuary deviates from equilibrium conditions with a semi-analytical global model for transport of SPM. The model, which operates at tidally-averaged timescale, solves the mass balance equation for SPM, namely,

$$\frac{\partial c}{\partial t} + \sum_{k=\{x,y,z\}} \frac{\partial F_k}{\partial k} = 0. \quad (1)$$

where

$$F_x = uc - K_h \frac{\partial c}{\partial x}, F_y = vc - K_h \frac{\partial c}{\partial y}, \text{ and } F_z = (w - w_s)c - K_v \frac{\partial c}{\partial z}, \quad (2)$$

with $\{x, y, z\}$ the three Cartesian directions, (u, v, w) the components of the three tridimensional current vector, K_h and K_v are, respectively, the horizontal and vertical turbulent diffusion coefficients, and w_s the sediment fall velocity.

Equation 1 is applied to the Guadalquivir estuary, segmented in $N = 6$ prismatic and laterally homogeneous boxes (volumes), defined by the locations of the CTDs, namely, $x_1 = 0 \text{ km}$, $x_2 = 17.3 \text{ km}$, $x_3 = 23.6 \text{ km}$, $x_4 = 26.2 \text{ km}$, $x_5 = 35.3 \text{ km}$, $x_6 = 47.1 \text{ km}$ and $x_7 = 57.6 \text{ km}$, where the origin of the along-channel coordinate (positive upstream) was established at the monitoring station, installed at the mouth

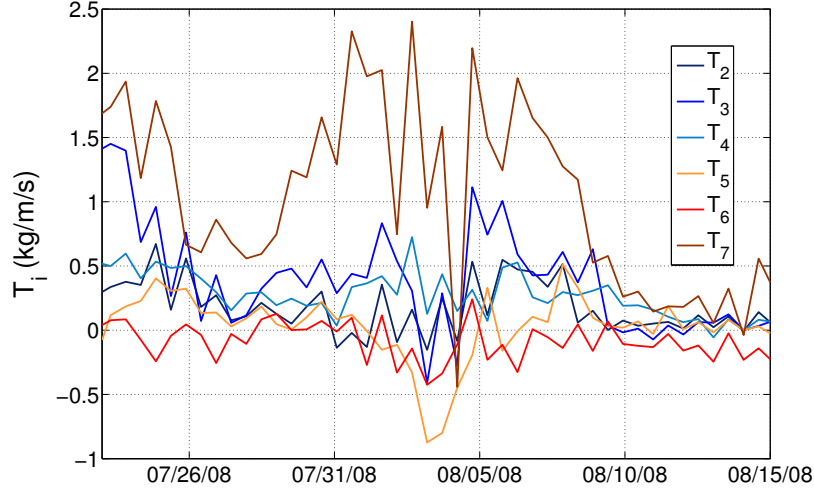


Figure 4: Time series of along-channel SPM transports (per unit width).

of the estuary. Imposing stationary conditions, and assuming no sediment fluxes from banks and surface, and that the total SPM mass, M , is conserved inside the estuary, a system of N linear equations with N unknowns is obtained.

$$\mathbf{G} \cdot \mathbf{y} = \mathbf{B}, \quad (3)$$

where \mathbf{B} is the column vector

$$\mathbf{B} = (M, b_3 T_3 - b_2 T_2, \dots, b_{N+1} T_{N+1} - b_N T_N)^t, \quad (4)$$

and \mathbf{G} is a matrix $N \times N$ whose elements G_{ji} are

$$G_{ji} = \begin{cases} 1 & \text{if } j = 1, \\ \frac{K_{h,i}}{(x_{i+1}-x_{i-1})(x_i-x_{i-1})} & \text{if } 1 \leq j-1 = i \leq N, \\ -\frac{K_{h,i}}{(x_{i+1}-x_{i-1})(x_{i+1}-x_i)} - \frac{K_{h,i+1}}{(x_{i+2}-x_i)(x_{i+1}-x_i)} & \text{if } 2 \leq j = i \leq N, \\ \frac{K_{h,i+1}}{(x_{i+2}-x_i)(x_{i+2}-x_{i+1})} & \text{if } 3 \leq j+1 = i \leq N. \end{cases} \quad (5)$$

Finally, \mathbf{y} is the $N \times 1$ unknown vector which contains the suspended sediment masses under stationary conditions at each volume i , \widehat{m}_i ,

$$\mathbf{y} = (\widehat{m}_1, \widehat{m}_2, \dots, \widehat{m}_{N+1})^t, \quad (6)$$

The variables of the above set of equations are nondimensionalized with $b_{\text{ref}} = 400$ m, $K_{\text{ref}} = 1.5 \cdot 10^3$ m²/s, $M_{\text{ref}} = 10^8$ kg, $L_{\text{ref}} = 110$ km, and $T_{\text{ref}} = 2K_{\text{ref}}M_{\text{ref}}/(b_{\text{ref}}L_{\text{ref}}^2) = 0.0620$ kg/m/s. These numbers represent typical values for width, dispersion coefficient, mass, estuary length and transport, respectively. The main inputs to Eq. 3 are the advective along-channel transport rates, $T_i = (h_0 + \eta_i) u_i c_i$ for $i = 2, \dots, N + 1$, estimated from the measurements at the CTDs locations, and the coefficients $K_{h,i}$. The transports at each tidal cycle for each stretch are shown in Fig. 4. The values $K_{h,i}$ employed are $K_{h,i} = 1754$ m²/s for $i = 5, 6$ and $K_{h,i} = 963$ m²/s for the rest of the boxes, similarly to those obtained for salinity in Díez-Minguito et al. (2013).

The application of this model to the Guadalquivir estuary allowed to check how the SPM concentrations in different control volumes or boxes of the estuary (differenced by colors in the upper part of Fig. 5) deviate from their equilibrium values. Figure 5, lower panel, compares the observed concentrations of SPM, m_i , with the modeled masses at equilibrium, \widehat{m}_i , at neap tide (08/10/08) and spring tide (08/03/08). The relative difference, $R_m = (\widehat{m}_i - m_i)/m_i$, provides a first indication of the deviation of the mass of suspended matter in each box from its equilibrium value. The results show that in the lower stretches there is a deficit of

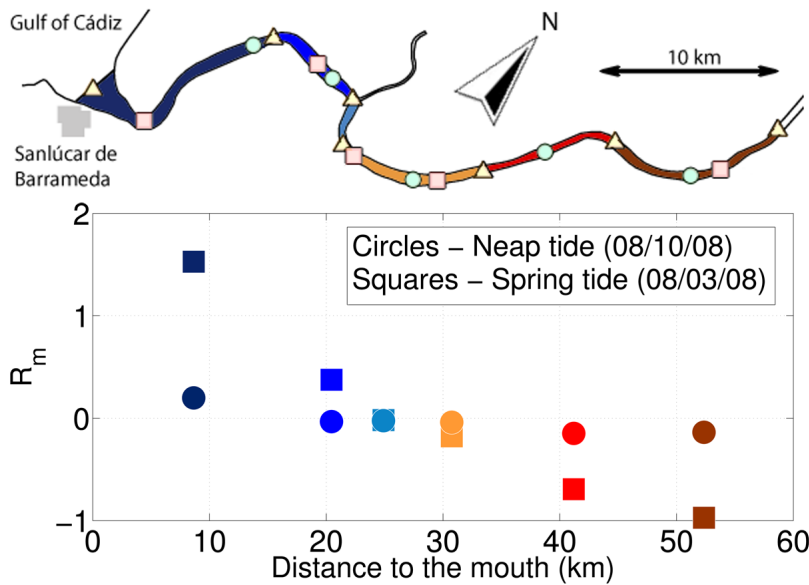


Figure 5: Top panel: Control volumes and instrumentation. Bottom panel: Relative SPM deficit in the water column, $R_m = (\widehat{m}_i - m_i) / m_i$ at neap and spring tide.

sediment, thus erosion is favored, whereas upstream stretches are in excess. During spring tides (squares) R_m amplifies, whereas during neap tides (circles) those differences tend to reduce. Therefore, the estuary seems to move towards equilibrium during weak tidal forcing conditions.

CONCLUSIONS

Turbidity in the Guadalquivir estuary is analyzed and discussed by using hydrodynamic data records collected during a comprehensive field survey over a 3 year period. The spatial distribution and sources of the suspended particulate matter are identified. Most of the sediment is kept in suspension by tidal action. Tidal straining seems to control the estuarine circulation both near the mouth and the saline intrusion null point. At subtidal time scales, the along-channel distribution of suspended sediment is not uniform, and exhibits two turbidity maxima. The deviation from morphodynamic equilibrium of the estuary is assessed using a simple box model. The results seem to indicate that erosion is dominant in the lower stretches and that the sediment tends to be transported upstream, where deposition is favored. Despite the simplifying assumptions (e.g. is not time-dependent), the model, as long as SPM transports are provided, can be used as a management aiding tool assessing the impact of planned human interventions. The model is flexible and fast, and yield insight into morphodynamics.

ACKNOWLEDGMENTS

This research was funded by Projects CTM2009-10520/MAR, P09-TEP-4630, and P09-RNM-4735, and a research contract between the University of Granada, the University of Córdoba, and the CSIC.

References

- H. Burchard and H. Baumert. The formation of estuarine turbidity maxima due to density effects in the salt wedge. a hydrodynamic process study. *Journal of Physical Oceanography*, 28(2):309–321, 1998.
- A. S. Chernetsky, H. M. Schuttelaars, and S. A. Talke. The effect of tidal asymmetry and temporal settling lag on sediment trapping in tidal estuaries. *Ocean Dynamics*, 60(5):1219–1241, 2010.
- E. Contreras and M. Polo. Measurement frequency and sampling spatial domains required to characterize turbidity and salinity events in the Guadalquivir estuary (Spain). *Natural Hazards and Earth System Science*, 12(8):2581–2589, 2012.

- M. Díez-Minguito, A. Baquerizo, M. Ortega-Sánchez, G. Navarro, and M. Losada. Tide transformation in the Guadalquivir estuary (SW Spain) and process-based zonation. *Journal of Geophysical Research*, 117 (C3):C03019, 2012.
- M. Díez-Minguito, E. Contreras, M. Polo, and M. Losada. Spatio-temporal distribution, along-channel transport, and post-riverflood recovery of salinity in the Guadalquivir estuary (SW Spain). *Journal of Geophysical Research*, 118(5):2267–2278, 2013.
- K. R. Dyer. Sediment transport processes in estuaries. *Developments in Sedimentology*, 53:423–449, 1995.
- D. A. Jay and J. D. Musiak. Particle trapping in estuarine tidal flows. *Journal of Geophysical Research*, 99 (C10):20445–20461, 1994.
- J. Lin and A. Y. Kuo. Secondary turbidity maximum in a partially mixed microtidal estuary. *Estuaries*, 24 (5):707–720, 2001.
- G. Navarro, F. J. Gutierrez, M. Díez-Minguito, M. A. Losada, and J. Ruiz. Temporal and spatial variability in the Guadalquivir Estuary: A challenge for real-time telemetry. *Ocean Dynamics*, 61(6):753–765, 2011.
- R. Pawlowicz, B. Beardsley, and S. Lentz. Classical tidal harmonic analysis including error estimates in MATLAB using T-TIDE. *Computers & Geosciences*, 28:929–937, 2002.
- M. Reyes-Merlo, M. Díez-Minguito, M. Ortega-Sánchez, A. Baquerizo, and M. Losada. On the relative influence of climate forcing agents on the saline intrusion in a well-mixed estuary: Medium-term Monte Carlo predictions. *Journal of Coastal Research*, 65:1200–1205, 2013.
- J. Ruiz, M. Polo, M. Díez-Minguito, G. Navarro, E. Morris, E. Huertas, I. Caballero, E. Contreras, and M. Losada. *The Guadalquivir estuary: A hot spot for environmental and human conflicts in Advances in Coastal and Marine Resources: Remote Sensing and Modeling*, (eds) Klein, A.H.F. and Finkl, C.W. Springer, 2014. in press.
- J. H. Simpson, J. Brown, J. Matthews, and G. Allen. Tidal straining, density currents, and stirring in the control of estuarine stratification. *Estuaries*, 13(2):125–132, 1990.
- S. A. Talke, H. E. de Swart, and V. N. de Jonge. An idealized model and systematic process study of oxygen depletion in highly turbid estuaries. *Estuaries and coasts*, 32(4):602–620, 2009.